

Mimic Human Cognition, Master Multi-Image Reasoning: A Meta-Action Framework for Enhanced Visual Understanding

Jianghao Yin^{1,2*}, Qingbin Li², Kun Sun², Cheng Ding¹, Jie Wang², Qin Chen^{1†}, Jie Zhou¹, Nan Wang², Changqing Li², Pei Wu², Jian Xu^{2†}, Zheming Yang², Liang He¹

¹East China Normal University ²ByteDance

Abstract

While Multimodal Large Language Models (MLLMs) excel at single-image understanding, they exhibit significantly degraded performance in multi-image reasoning scenarios. Multi-image reasoning presents fundamental challenges including complex inter-relationships between images and scattered critical information across image sets. Inspired by human cognitive processes, we propose the Cognition-Inspired Meta-Action Framework (CINEMA), a novel approach that decomposes multi-image reasoning into five structured meta-actions: Global, Focus, Hint, Think, and Answer which explicitly modeling the sequential cognitive steps humans naturally employ. For cold-start training, we introduce a Retrieval-Based Tree Sampling strategy that generates high-quality meta-action trajectories to bootstrap the model with reasoning patterns. During reinforcement learning, we adopt a two-stage paradigm: an exploration phase with Diversity-Preserving Strategy to avoid entropy collapse, followed by an annealed exploitation phase with DAPO to gradually strengthen exploitation. To train our model, we construct a dataset of 57k cold-start and 58k reinforcement learning instances spanning multi-image, multi-frame, and single-image tasks. We conduct extensive evaluations on multi-image reasoning benchmarks, video understanding benchmarks, and single-image benchmarks, achieving competitive state-of-the-art performance on several key benchmarks. Our model surpasses GPT-4o on the MUIR and MVMATH benchmarks and notably outperforms specialized video reasoning models on video understanding benchmarks, demonstrating the effectiveness and generalizability of our human cognition-inspired reasoning framework.

1. Introduction

Multimodal Large Language Models (MLLMs) have demonstrated remarkable capabilities in single-image understanding tasks [3, 11, 28, 38, 67], with extensive research focusing on enhancing models’ single-image reasoning abilities [6, 25, 72, 79]. However, real-world applications often involve processing multiple images simultaneously, such as in e-commerce, autonomous driving, and video content understanding. Despite their success in single-image tasks, MLLMs exhibit degraded performance when handling multi-image reasoning scenarios [54, 66].

Multi-image reasoning presents two fundamental challenges. First, images often exhibit complex inter-relationships: semantic associations, spatial arrangements, temporal sequences, that are crucial for task completion yet require sophisticated integration beyond isolated image processing [54, 89]. Second, critical information may be scattered across specific images within larger sets, demanding precise identification and focus on relevant visual content while filtering out distractors.

Human cognition offers valuable insights for these challenges. When approaching complex multi-image reasoning tasks, humans employ a systematic process grounded in established cognitive principles. Research shows that humans effectively integrate both global structures and local details during visual perception [52, 55], enabling comprehensive problem understanding across multiple levels. Additionally, studies demonstrate that explicitly identifying and articulating key information significantly enhances performance on complex reasoning tasks [13]. This natural cognitive process suggests that artificial reasoning systems would benefit from cognitive frameworks that explicitly model these human-like reasoning patterns.

Motivated by these observations, we propose the **Cognition-Inspired Meta-Action Framework (CINEMA)** that addresses multi-image reasoning through three key in-

[†]Corresponding Authors.

^{*}Work done during internship at ByteDance.

novations. First, we introduce a set of five meta actions: Global, Focus, Hint, Think, and Answer, which systematically guide models through human-inspired reasoning processes. These meta actions provide a structured cognitive framework that enables models to effectively navigate the complexities of multi-image reasoning by explicitly modeling the sequential cognitive steps that humans naturally employ. Second, we develop a Retrieval-Based Tree Sampling strategy that mirrors human learning dynamics through a student-teacher paradigm. This approach generates diverse, high-quality reasoning trajectories by first allowing a student model to attempt initial solutions, then having a teacher model refine these attempts, and finally retrieving alternative solution paths from a database of reasoning trajectories. This process not only ensures the quality of training data but also refines the reasoning trajectories, enabling the model to generate reasoning patterns that more closely resemble human-like thinking. Third, we design a novel two-stage reinforcement learning approach to optimize the reasoning process while maintaining trajectory diversity. We observe that standard reinforcement learning often suffers from entropy collapse [14, 40, 71], where policies become overly deterministic and lose exploration capacity over time. To address this challenge, our first stage employs **Diversity-Preserving Strategy (DPS)** with a trajectory homogeneity penalty to maintain sufficient exploration and prevent premature convergence to suboptimal solutions. The second stage then applies decoupled clip and dynamic sampling policy optimization (DAPO) [84] to gradually transition toward more focused behaviors, effectively balancing the exploration-exploitation trade-off throughout the training process.

To train our model, we construct a high-quality training dataset comprising 57k cold-start instances and 58k reinforcement learning instances. Each cold-start instance contains two distinct reasoning trajectories to provide diverse supervision signals during initial training. The dataset encompasses three categories of visual reasoning tasks: multi-image tasks, multi-frame tasks and single-image tasks. Our main contributions are as follows:

- We propose a human cognition-inspired reasoning framework that decomposes complex multi-image reasoning into five structured meta actions (Global, Focus, Hint, Think, Answer). This framework systematically models the sequential cognitive processes that humans naturally employ when solving multi-image reasoning tasks, providing explicit guidance for models to navigate complex visual reasoning scenarios.
- We introduce a novel Retrieval-Based Tree Sampling strategy that generates diverse, high-quality training trajectories through student-teacher interactions, coupled with a two-stage reinforcement learning paradigm: Diversity-Preserving Strategy with trajectory homogeneity

penalty to maintain exploration, followed by DAPO to consolidate performance while preserving learned diversity.

- We construct a comprehensive training dataset with 57k cold-start instances where each contains two reasoning trajectories, and 58k reinforcement learning instances across multi-image, multi-frame, and single-image tasks.
- We conduct extensive evaluations across multiple benchmarks spanning multi-image reasoning, video understanding, and single-image tasks. Our method achieves state-of-the-art performance on numerous benchmarks and notably outperforms specialized video reasoning models on video understanding tasks, demonstrating the effectiveness and generalizability of our approach.

2. Related Work

Multimodal Reasoning. Recent works have enhanced MLLM reasoning capabilities [15, 24, 25, 61, 78], but most focus on single-image scenarios. Real-world applications like autonomous driving and video understanding require multi-image reasoning. Existing multi-image approaches have key limitations. Zhang et al. [89] propose a Focus-Centric Visual Chain that decomposes multi-image tasks into sequential sub-questions targeting specific visual subsets. However, their reasoning process mainly focuses on individual image subsets instead of leveraging global multi-image context. MIA-DPO [47] augments single-image datasets with unrelated images for preference optimization, but primarily handles cases where questions involve only single images within multi-image contexts. Authentic multi-image reasoning requires models to analyze individual images while comprehending holistic relationships among all images. Inspired by human cognition, we propose a reasoning framework that effectively navigates both local image analysis and global inter-image relationships.

Reinforcement Learning for Reasoning and Entropy Control. Early reinforcement learning approaches for foundation models relied on Reinforcement Learning from Human Feedback (RLHF), which required training a separate reward model and extensive human-labeled preference data [27, 56]. Direct Preference Optimization (DPO) [58] simplified this pipeline but still depended on preference annotations. More recently, large-scale pure RL methods have shown strong gains in reasoning, with outcome-based rewards alone proving effective [7, 18, 22, 46, 65, 77, 86]. To regulate exploration, many approaches add entropy or KL regularization [20, 45], introduce entropy bonuses through reward shaping [12], or apply stabilizing heuristics such as loss reweighting [14, 71] and clip-higher mechanisms [84]. While these methods focus on entropy within a single response, others encourage diversity across responses, e.g.,

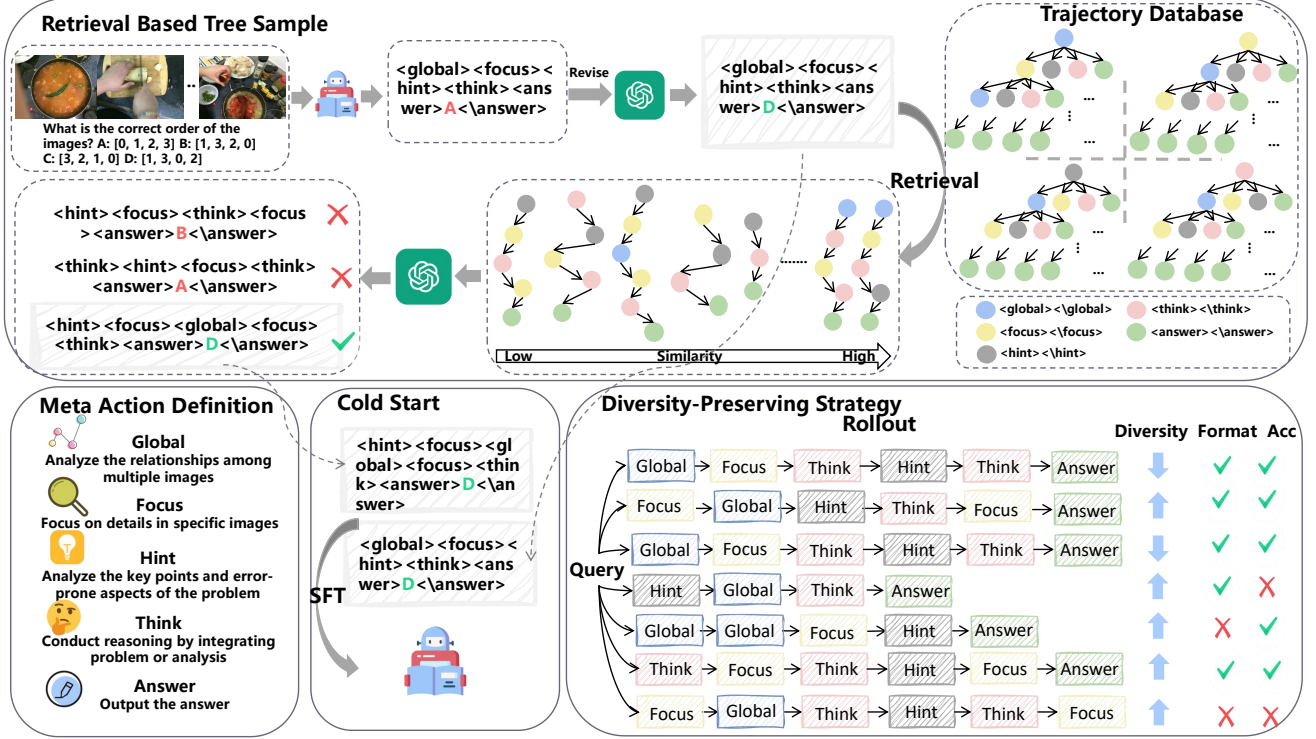


Figure 1. Overview of CINEMA.

via embedding-based distance measures [10] or enforcing dissimilarity in generated answers [8]. Our approach builds on this line of work but emphasizes diversity at the meta-action level for entropy control.

3. Method

The framework of our method is shown in Figure 1. We first define five structured meta actions: Global, Focus, Hint, Think, and Answer, which model human cognitive processes (Section 3.1). We then propose Retrieval-Based Tree Sampling to generate diverse, high-quality training trajectories via student-teacher interactions (Section 3.2), and construct a comprehensive dataset with 57k cold-start and 58k reinforcement learning instances (Section 3.3). Finally, we introduce a two-stage training paradigm: in the first stage, Diversity-Preserving Strategy prevents entropy collapse and maintains trajectory diversity during reinforcement learning, and in the second stage, DAPO anneals the policy toward exploitation to consolidate performance (Section 3.4).

3.1. Meta Action Definition

Global. This meta action simulates how humans typically approach complex problems by first reading through the entire question to grasp its overall structure. When dealing with multi-image input tasks, there may be temporal, spatial, semantic, or other relationships between the im-

ages. This action helps the model identify and leverage these inter-image dependencies to enhance understanding and reasoning.

Focus. This meta action simulates how humans tackle complex problems by concentrating on analyzing key information relevant to the question. In the context of multi-image reasoning, critical clues may reside in a specific image. The model should therefore focus its analysis on that image and pay close attention to salient visual details.

Hint. This meta action simulates how humans improve accuracy by summarizing key points and error-prone aspects of a problem when solving tasks. In multi-image reasoning tasks, similarly, there often exists misleading or easily confusable information between images.

Think. This meta action simulates how humans engage in internal reasoning by actively processing acquired information to formulate solutions or hypotheses. It involves analyzing the relationships between provided clues, leveraging prior knowledge, and performing logical inference.

Answer. This meta action outputs the final answer based on all prior analytical insights and reasoning outcomes. It is the final action in the compliant trajectory.

3.2. Retrieval Based Tree Sample

To effectively leverage the defined meta actions for multi-image reasoning enhancement, we propose a novel cold-

start data sampling strategy called Retrieval-Based Tree Sampling. This approach is inspired by human learning mechanisms, where students first attempt problems independently before receiving guidance from teachers who first refine their initial approach and then introduce alternative solution pathways.

With the meta actions defined in Section 3.1, we maintain several meta action trees, each containing multiple reasoning trajectories. Every trajectory in these trees terminates with the `Answer` meta action, forming complete reasoning paths from problem comprehension to solution derivation. These trees serve as a database of diverse reasoning strategies that can be retrieved and adapted for new problems. The Retrieval-Based Tree Sampling process is shown as follows:

Step 1. Initial Trajectory Generation. We first prompt a smaller model (student model) to perform initial reasoning on the given task using meta actions. This generates an initial trajectory regardless of whether the final answer is correct or incorrect. This step mirrors how students first attempt to solve problems using their existing knowledge and reasoning patterns.

Step 2. Teacher-Guided Trajectory Refinement. The initial trajectory from Step 1 is then provided to a stronger model (GPT-4o, serving as the teacher model). The teacher model follows the student’s reasoning action trajectories and reason again, similar to how human teachers guide students by first understanding their thought processes and then providing corrections. This produces a correct trajectory that maintains the original action trajectories while ensuring accuracy.

Step 3. Retrieval-Based Diverse Sampling. To enrich the learning experience and expand the exploration space for subsequent reinforcement learning, we perform retrieval-based sampling from our trajectory tree database. Starting from trajectories with low similarity to the initial trajectory from Step 2, we progressively search through increasingly similar trajectories until we identify an alternative correct reasoning path. This process ensures that each training instance is associated with two distinct correct trajectories.

3.3. Dataset Construction

To train our model, we construct a high-quality training dataset that supports both cold-start initialization and reinforcement learning phases. Our dataset encompasses three primary categories: multi-image tasks in which the number of input images is at least two, multi-frame tasks that involve reasoning over sequential frames from videos or time-series visual data, and single-image tasks that the number of input image is only one. All the data is obtained through existing open-source multi-modal datasets. More details about dataset is shown in Appendix 9.

The key distinction between our cold-start and reinforcement learning dataset splits lies in the trajectory generation process described in Section 3.2. Cold-start training data consists of problems where GPT-4o successfully provides correct answers during Step 2, and for these instances, we proceed to Step 3 (retrieval-based diverse sampling) to obtain two distinct correct reasoning trajectories per problem that serve as supervised learning targets for cold start training. In contrast, reinforcement learning data comprises problems where GPT-4o fails to produce correct answers during Step 2, and these challenging cases are reserved for reinforcement learning.

3.4. Balancing Exploration and Exploitation via Two-Stage Optimization

A critical challenge in reinforcement learning for reasoning is policy entropy collapse which limits exploration and generalization capacity. We address this through a two-stage training paradigm: first maintaining trajectory diversity to preserve exploration, then gradually shifting toward exploitation to consolidate performance.

Diversity-Preserving Strategy. In the first stage, we aim to prevent entropy collapse by maintaining diversity at the meta-action level. To this end, we propose Diversity-Preserving Strategy(DPS) which is built on DAPO [84] (more details about DAPO is shown in Appendix 7). Our central hypothesis is that encouraging a variety of solution strategies can better leverage the model’s potential and improve its generalization performance like human.

We operationalize this by promoting diverse responses for questions that the model answers correctly. To this end, we define the reward as a weighted combination of accuracy and format validity:

$$R = 0.5 \cdot \left[R_{\text{acc}} \cdot \left(R_{\text{acc}} - \frac{N-1}{G-1} \cdot 0.1 \right) \right] + 0.5 \cdot R_{\text{format}}, \quad (1)$$

where R_{acc} and R_{format} are binary indicators:

$$R_{\text{acc}} = \begin{cases} 1, & \text{if the answer is correct,} \\ 0, & \text{otherwise,} \end{cases} \quad R_{\text{format}} = \begin{cases} 1, & \text{if all meta actions in the response are valid,} \\ 0, & \text{otherwise.} \end{cases} \quad (2)$$

Here, G denotes the group size used in sampling, and N represents the number of trajectories within the group that share identical meta-action patterns. Intuitively, the penalty term $\frac{N-1}{G-1}$ discourages over-reliance on homogeneous trajectories, thereby encouraging the model to maintain diversity across solutions. This design ensures that correct answers are not only accurate but also exhibit a broad spectrum of solution strategies, thereby enhancing the model’s generalization. In practice, to perform dynamic sampling as

in DAPO, we use R_{acc} as the filtering criterion rather than the combined reward R .

Annealed Exploitation. In the second stage, we employ DAPO with an annealing schedule to gradually shift from exploration to exploitation, leveraging the diversity obtained in stage one while consolidating performance gains. This two-stage approach maintains higher entropy levels throughout training compared to standard methods, as validated by our Pass@K experiments.

4. Experiment Setup

4.1. Benchmark and Baselines

Benchmark. To ensure a comprehensive evaluation, we examine the performance of our method across a broad spectrum of benchmarks, encompassing both multi-image and single-image types. Specifically, for multi-image evaluations, we cover **multi-image comprehensive benchmarks** (including MUIR [66], MMIU [54], and Mantis-Eval [31]), **multi-image reasoning benchmarks** (including MV-MATH [69], MIRB [90] and EMMA [19]), **video comprehensive benchmarks** (including MV-Bench [39], and VideoMME [17]) and **video reasoning benchmarks** (including VideoMMU [23]). For single-image evaluations, we include **single-image comprehensive benchmarks** (including MMMU-Pro [85] and M3COT [9]) as well as **mathematics reasoning benchmarks** (including MM-Math [63], Math-Vision [68], and MathVista [51]). Accuracy is reported as the metric for all these benchmarks.

Baselines. We compare our method’s against four categories of models: closed-source MLLMs, including GPT-4V [1], Gemini-1.5-Pro [64], and GPT-4o [28]; open-source general-purpose MLLMs, including OpenFlamingo-v2 [2], LLaVAv1.6 [44], VILA1.5 [41], LLaVA-OneVision [35], InternVL2.5 [11], and Qwen2.5-VL [3]; and multi-image/video enhanced models, including Mantis-Idefics [31], mPLUG-Owl3 [82], LLaVA-NeXT-Interleave [36], CMMCOT [88], MIA-DPO [47], VISC [89], VideoR1 [16], and VideoRFT [70]; Single-image reasoning models: Mulberry 7B [80], R1-Onenvision 7B [79], VLAA-Thinker 7B [6], VisonR1 7B [25], MixedR1 7B [75].

4.2. Implementation Details

We select Qwen2.5VL 7B as our backbone model. During the cold-start training phase, the model is trained for two epochs with a learning rate of 1×10^{-5} . We employ a two-stage reinforcement learning procedure. The first stage consists of 700 steps of DPS-based entropy enhancement, followed by 300 steps of DAPO-based annealed exploitation. In the subsequent reinforcement learning stage, both the KL-divergence and entropy regularization terms are omitted. Rollouts are generated using a batch size of 64, a temperature of 1.0, and 8 rollouts per prompt. For policy opti-

mization, an update batch size of 32 is adopted. Regarding reward design, we incorporate domain-specific validation mechanisms: `math_verify` [34] and `mathruler` [21] are employed to evaluate answers in mathematical problem-solving, whereas exact string matching is applied to non-mathematical tasks. To ensure structural consistency, format rewards are introduced by imposing constraints on the response space, requiring outputs to conform to a valid meta-action trajectory. Specifically, for single-image inputs, the `global` action is disallowed, whereas for multi-image inputs, the inclusion of the `global` action is mandatory. During inference, we set the decoding hyperparameters as follows: temperature = 0.6, top- p = 0.7, and a maximum of 1024 generated tokens. Additional implementation details are provided in the Appendix 10.

5. Experiments

5.1. Results on multi-image Benchmark

Table 1 presents the experimental results on multi-image benchmarks, where our model demonstrates significant improvements over Qwen2.5VL across all benchmarks, achieving state-of-the-art performance on MUIR, MVMATH, EMMA, VideoMME, and VideoMMU benchmarks. Remarkably, our model surpasses the closed-source GPT-4o on both MUIR and MVMATH benchmarks. On multi-image comprehensive benchmarks, our model achieves 13.7% improvement over Qwen2.5VL on the MUIR benchmark and 6.9% improvement on MIRB. These multi-image benchmarks encompass diverse multi-image tasks, demonstrating our model’s robust capability in processing multi-image inputs. On multi-image reasoning benchmarks, MVMATH is a mathematics dataset with multi-image inputs, while EMMA encompasses multiple academic disciplines. These benchmarks require strong reasoning capabilities from the model. Our model achieves 10.2% improvement on MVMATH and 8.9% improvement on EMMA, reflecting enhanced reasoning capabilities attributed to CINEMA, which simulates human-like reasoning processes through structured meta-action trajectory and cross-image relationship modeling. Notably, our model surpasses specialized video reasoning models across all three video benchmarks, despite not being specifically designed for video reasoning tasks. This demonstrates our model’s superior performance in handling temporal multi-image data, suggesting that our approach effectively captures both spatial and temporal dependencies inherent in sequential visual information.

5.2. Results on single-image Benchmark

Table 2 presents the results on single-image benchmarks, where our model demonstrates equally strong capabilities. Our model achieves superior overall performance compared to existing models specifically designed for single-image

Model	MUIR	MMIU	MVMATH	EMMA	MIRB	Mantis	MV Bench	VideoMME	VideoMMU	Overall
<i>Closed-Source MLLMs</i>										
<i>Open-Source General MLLMs</i>										
OpenFlamingo-v2 9B	22.3	23.7	-	-	28.8	12.4	7.9	-	-	-
LLaVA 1.6 7B	27.4	22.2	-	-	29.8	45.6	40.9	-	-	-
VILA1.5 8B	33.1	32.5	-	-	36.5	51.2	49.4	20.9	-	-
LLaVA-OneVision 7B	41.8	40.3	19.1	-	51.2	64.2	56.7	-	-	-
InternVL2.5 8B	51.1	46.7	18.8	21.0	52.5	67.7	72.0	56.1	35.2	46.8
Qwen2.5-VL-7B	57.9	50.6	26.7	20.4	48.3	64.5	62.6	56.7	45.8	48.2
<i>Multi-image/Video Enhancing MLLMs</i>										
Mantis-Idfics2 8B	44.5	45.6	15.5	20.3	34.8	57.1	51.4	42.6	19.3	36.8
LLaVA-NeXT-Interleave 7B	31.1	47.3	14.7	19.0	39.3	62.7	53.1	47.2	23.2	37.5
mPLUG-Owl3 8B	34.0	39.7	18.7	24.8	41.2	63.1	54.5	53.5	32.0	40.2
MIA-DPO 7B	-	-	-	-	-	60.4	63.6	-	-	-
CcDPO 7B	44.8	-	-	-	-	60.7	69.1	-	-	-
VISC 7B	44.5	52.8	-	-	60.2	69.1	68.0	-	-	-
VideoR1 7B	-	-	-	-	-	-	63.6	57.4	49.8	-
VideoRFT 7B	56.6	44.5	25.1	17.8	46.7	56.7	62.1	59.8	51.1	46.7
TW-GRPO 7B	55.9	44.9	28.2	22.5	24.3	49.8	63.3	55.1	40.8	42.8
Ours	71.6	53.3	36.9	29.3	55.2	67.7	66.5	59.4	49.0	54.3
Δ (vs Qwen2.5VL 7B)	+13.7	+2.7	+10.2	+8.9	+6.9	+3.2	+3.9	+2.7	+3.2	+6.1
Ours [with DPS]	67.9	52.2	35.1	28.4	54.4	71.0	67.1	60.2	51.6	54.2
Δ (vs Qwen2.5VL 7B)	+10.0	+1.6	+8.4	+8.0	+6.1	+6.5	+4.5	+3.5	+5.8	+6.0
Ours [with DPS and annealing]	71.0	52.2	35.0	28.6	55.7	68.4	66.8	61.0	50.1	54.3
Δ (vs Qwen2.5VL 7B)	+13.1	+1.6	+8.3	+8.2	+7.4	+3.9	+4.2	+4.3	+4.3	+6.1

Table 1. Performance on multi-image/video benchmark. Ours indicates training with DAPO, Ours [with DPS] indicates training with DPS, and Ours [with DPS and annealing] indicates training with two-stage RL, where all models are trained for the same steps.

reasoning, despite being trained on only a limited amount of single-image data. This validates the generalizability of our approach, proving its effectiveness not only for multi-image scenarios but also for single-image tasks. On comprehensive single-image benchmarks, our model achieves 3% improvement on MMMU-Pro and 3.8% improvement on M3COT, surpassing the closed-source models GPT-4V and GPT-4o on M3COT. On math benchmarks, our model attains state-of-the-art performance on MM-Math and achieves comparable performance to existing models specialized in single-image reasoning across other mathematical benchmarks.

5.3. Results on Pass@K Setting

To further validate the advantages of our proposed two-stage RL approach, we conduct Pass@K experiments on 7 multi-image and 7 single-image benchmarks, comparing models with and without DPS and annealing. We evaluate the accuracy across K inference attempts, where $K \in 2, 4, 8, 16$, and a model is considered correct if at least one inference attempt produces the correct answer. We report the average accuracy in Figure 2. The results show that

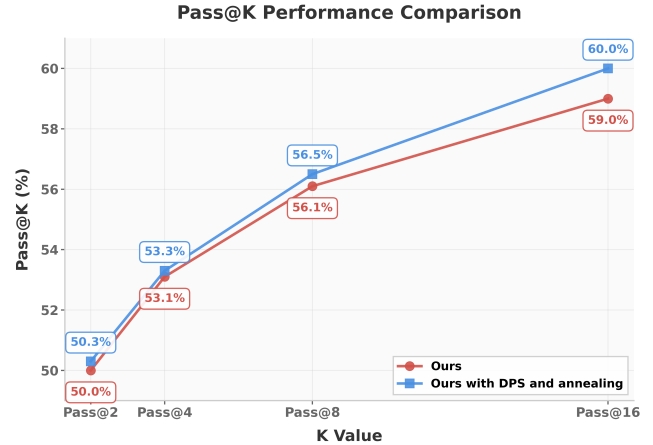


Figure 2. Pass@K performance.

incorporating two-stage RL consistently outperforms the baseline across pass@2, pass@4, pass@8, and pass@16, further demonstrating the effectiveness of our two-stage RL method. After this training paradigm, the model exhibits more diverse sampling behavior and achieves a higher per-

Model	MMMU-Pro	M3COT	MM-IQ	MM-Math	Math-Vision	MathVista	MathVerse	Overall
<i>Closed-Source MLLMs</i>								
GPT-4V	-	62.60	-	23.1	22.76	49.9	39.4	-
Gemini-1.5-Pro	51.47	-	26.86	-	-	-	-	-
GPT-4o	56.13	55.7	26.87	31.8	-	-	-	-
<i>Open-Source General MLLMs</i>								
LLaVA-OneVision 7B	-	-	-	-	-	63.2	26.2	-
InternVL2.5 8B	34.3	-	-	-	22.0	64.4	39.5	-
Qwen2.5VL 7B	38.0	60.1	26.1	36.4	19.5	65.3	40.4	40.8
<i>Reasoning MLLMs</i>								
Mulberry	-	-	-	23.7	-	63.1	-	-
R1-Onevision 7B	33.9	57.3	25.1	32.9	29.9	64.1	46.4	41.4
VLAA-Thinker 7B	39.5	61.3	26.3	39.0	26.4	68.0	47.8	44.0
VisonR1 7B	30.3	53.2	24.3	40.0	29.9	73.5	52.4	43.4
MixedR1 7B	38.0	59.9	25.9	35.8	30.3	70.6	40.8	43.0
Ours	40.6	63.5	25.6	43.8	26.7	68.7	49.4	45.5
Δ (vs Qwen2.5VL 7B)	+2.6	+3.4	+0.5	+7.4	+7.2	+3.4	+9.0	+4.7
Ours [with DPS]	40.7	63.9	26.3	43.4	26.1	70.0	47.6	45.4
Δ (vs Qwen2.5VL 7B)	+2.7	+3.8	+0.2	+7.0	+6.6	+4.7	+7.2	+4.6
Ours [with DPS and annealing]	41.0	62.7	27.3	43.4	26.1	70.1	48.5	45.6
Δ (vs Qwen2.5VL 7B)	+3.0	+2.6	+1.2	+7.0	+6.6	+4.8	+8.1	+4.8

Table 2. Performance on single-image benchmark. Ours indicates training with DAPO, Ours [with DPS] indicates training with DPS, and Ours [with DPS and annealing] indicates training with two-stage RL.

formance ceiling.

Method	MUIR	MMIU	EMMA	
Original	57.9	50.6	20.4	
Direct Prompting	33.8	36.9	14.1	
	SFT	RL	SFT	RL
Conventional CoT	59.0	70.0	49.9	51.6
Single Trajectory	56.3	65.1	50.9	52.2
Ours (Two Traj.)	58.2	71.6	51.9	53.3
				24.8
				29.3

Table 3. Ablation study on Retrieval-Based Tree Sampling.

5.4. Further analysis

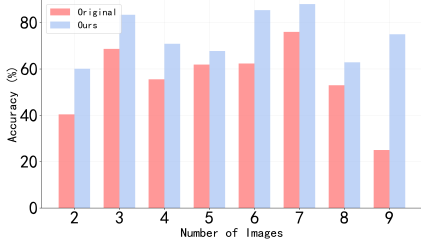
To conduct an in-depth analysis of our model, we propose 5 research questions and conduct detailed experiments:

RQ1: Can diverse trajectories improve model performance? To validate the effectiveness of our proposed Retrieval-Based Tree Sampling strategy, which samples two different trajectories for each data point, we conduct comparative experiments on three benchmarks: MUIR, MMMU and EMMA. We compare against three baselines: (1) cold start training with only one trajectory then RL; (2) cold start training with conventional Chain-of-Thought (CoT) in the format of: <think>reasoning here</think><answer>answer</answer> then RL; and (3) directly prompting MLLMs to perform rea-

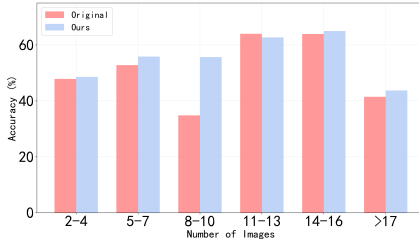
soning using meta actions without additional training. The experimental results are shown in Table 3. The model trained with two trajectories achieves superior average performance compared to models trained with single trajectories and conventional CoT training. Moreover, the best results under RL are all achieved by the model trained with two trajectories. In comparison to the directly prompted model, we observe that the untrained model performs poorly in utilizing our defined meta actions, showing significant performance degradation relative to the original model. This demonstrates the necessity of constructing datasets for subsequent training.

RQ2: How does the model perform with different numbers of input images? To investigate our model's capability in processing varying numbers of images, we conduct experiments on MUIR and MMIU benchmarks. The MUIR dataset contains samples with 2-9 input images per instance, whereas MMMU contains samples with 2-32 input images per instance. The experimental results are presented in Figures 3a and 3b. For different numbers of input images, our model outperforms the base model in most cases. Even when the number of input images exceeds 17, our model still achieves a significant improvement. This demonstrates the strong capability of our model in handling multi-image inputs and validates the effectiveness of the proposed cognition-inspired reasoning framework.

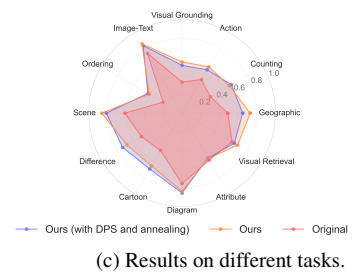
RQ3: How does the model perform across different tasks? To explore the performance of our model across dif-



(a) Results on MUIR.

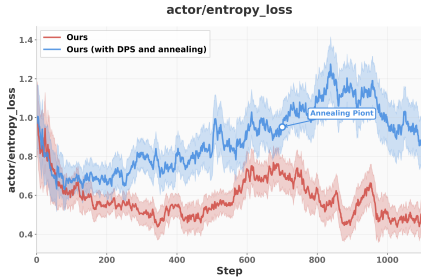


(b) Results on MMIU.

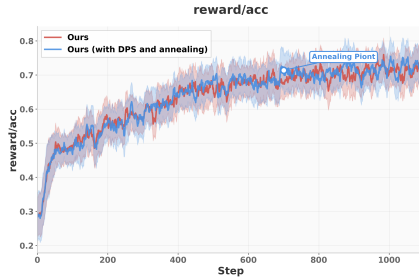


(c) Results on different tasks.

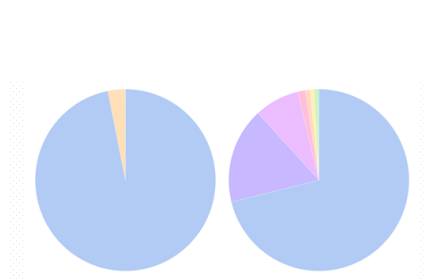
Figure 3. Results about RQ2 and RQ3.



(a) Entropy loss comparison.



(b) Reward comparison.



(c) Trajectory diversity comparison.

Figure 4. Results about RQ5.

ferent tasks, we present the results on MUIR, which consists of 12 distinct tasks, in Figure 3c. Our model achieves improvements on almost all tasks. Notably, tasks such as Geographic, Cartoon, and Visual Grounding were not included in our training set, yet our model still yields significant improvements on these tasks. This further demonstrates the generalization ability of our proposed reasoning framework in multi-image tasks.

RQ4: Whether each meta-action plays a role in our framework? To demonstrate the contribution of each meta action in our framework, we conduct ablation studies by individually removing `<global>`, `<focus>`, `<hint>`, and `<think>` from CINEMA, and evaluate the performance on MUIR, MIRB, and VideoMME (with the performance showing in Table 4). The results show that removing any of the actions leads to performance degradation, indicating that each meta-action plays an essential role in CINEMA.

Method	MUIR	MIRB	VideoMME
Ours	71.0	55.7	61.0
w/o global	63.4	52.6	57.1
w/o focus	61.6	53.2	57.5
w/o hint	63.5	52.3	56.8
w/o think	60.1	53.6	57.1

Table 4. Ablation study on meta actions.

RQ5: How does two-stage RL training influence en-

tropy and training dynamics? Figure 4a and 4b illustrate the effect of two-stage RL training on entropy and learning dynamics. In the first stage, diversity-preserving strategy maintains moderate entropy, which then gradually declines during the second annealing stage. Compared to the baseline, our method consistently preserves higher entropy levels, effectively averting entropy collapse. This sustained entropy promotes continued exploration, prevents premature convergence, and helps retain a diverse set of meta-actions. Notably, despite the higher entropy, our approach matches the baseline in training accuracy, confirming that the entropy-preserving mechanism does not compromise performance. Figure 4c visualizes the trajectories, where each color denotes a distinct trajectory type. The right plot (with two-stage RL) exhibits richer and more varied meta-action trajectories than the left (without), demonstrating that our method sustains policy diversity even after annealing. The improved performance is further validated by the Pass@K results in Figure 2.

6. Conclusion

In this work, we introduce CINEMA, a cognition-inspired meta-action framework that systematically decomposes multi-image reasoning into structured cognitive steps. By leveraging Retrieval-Based Tree Sampling for cold-start training and a two-stage reinforcement learning paradigm with diversity-preserving strategy and annealed DAPO, our approach effectively improve multi-image rea-

soning ability. Extensive experiments across multi-image, video, and single-image benchmarks demonstrate that CINEMA not only achieves state-of-the-art performance, surpassing even large general-purpose models such as GPT-4o in some key benchmarks, but also maintains higher policy diversity and adaptability. These results highlight the effectiveness, scalability, and generalizability of our framework, paving the way toward more robust multimodal reasoning systems.

References

[1] Josh Achiam, Steven Adler, Sandhini Agarwal, Lama Ahmad, Ilge Akkaya, Florencia Leoni Aleman, Diogo Almeida, Janko Altenschmidt, Sam Altman, Shyamal Anadkat, et al. Gpt-4 technical report. *arXiv preprint arXiv:2303.08774*, 2023. 5

[2] Anas Awadalla, Irena Gao, Josh Gardner, Jack Hessel, Yusuf Hanafy, Wanrong Zhu, Kalyani Marathe, Yonatan Bitton, Samir Gadre, Shiori Sagawa, et al. Openflamingo: An open-source framework for training large autoregressive vision-language models. *arXiv preprint arXiv:2308.01390*, 2023. 5

[3] Shuai Bai, Keqin Chen, Xuejing Liu, Jialin Wang, Wenbin Ge, Sibo Song, Kai Dang, Peng Wang, Shijie Wang, Jun Tang, et al. Owen2. 5-vl technical report. *arXiv preprint arXiv:2502.13923*, 2025. 1, 5

[4] Ankan Bansal, Yuting Zhang, and Rama Chellappa. Visual question answering on image sets. In *European Conference on Computer Vision*, pages 51–67. Springer, 2020. 3

[5] Jie Cao and Jing Xiao. An augmented benchmark dataset for geometric question answering through dual parallel text encoding. In *Proceedings of the 29th international conference on computational linguistics*, pages 1511–1520, 2022. 3

[6] Hardy Chen, Haoqin Tu, Fali Wang, Hui Liu, Xianfeng Tang, Xinya Du, Yuyin Zhou, and Cihang Xie. Sft or rl? an early investigation into training r1-like reasoning large vision-language models. *arXiv preprint arXiv:2504.11468*, 2025. 1, 5

[7] Huayu Chen, Kaiwen Zheng, Qinsheng Zhang, Ganqu Cui, Yin Cui, Haotian Ye, Tsung-Yi Lin, Ming-Yu Liu, Jun Zhu, and Haoxiang Wang. Bridging supervised learning and reinforcement learning in math reasoning. *arXiv preprint arXiv:2505.18116*, 2025. 2

[8] Minghan Chen, Guikun Chen, Wenguan Wang, and Yi Yang. Seed-grpo: Semantic entropy enhanced grpo for uncertainty-aware policy optimization. *arXiv preprint arXiv:2505.12346*, 2025. 3

[9] Qiguang Chen, Libo Qin, Jin Zhang, Zhi Chen, Xiao Xu, and Wanxiang Che. M3cot: A novel benchmark for multi-domain multi-step multi-modal chain-of-thought. In *Proceedings of the 62nd Annual Meeting of the Association for Computational Linguistics (Volume 1: Long Papers)*, pages 8199–8221, 2024. 5, 2, 3

[10] Xiwen Chen, Wenhui Zhu, Peijie Qiu, Xuanzhao Dong, Hao Wang, Haiyu Wu, Huayu Li, Aristeidis Sotiras, Yalin Wang, and Abolfazl Razi. Dra-grpo: Exploring diversity-aware reward adjustment for r1-zero-like training of large language models. *arXiv preprint arXiv:2505.09655*, 2025. 3

[11] Zhe Chen, Weiyun Wang, Yue Cao, Yangzhou Liu, Zhangwei Gao, Erfei Cui, Jinguo Zhu, Shenglong Ye, Hao Tian, Zhaoyang Liu, et al. Expanding performance boundaries of open-source multimodal models with model, data, and test-time scaling. *arXiv preprint arXiv:2412.05271*, 2024. 1, 5

[12] Daixuan Cheng, Shaohan Huang, Xuekai Zhu, Bo Dai, Wayne Xin Zhao, Zhenliang Zhang, and Furu Wei. Reasoning with exploration: An entropy perspective. *arXiv preprint arXiv:2506.14758*, 2025. 2

[13] Michelene TH Chi, Nicholas De Leeuw, Mei-Hung Chiu, and Christian LaVancher. Eliciting self-explanations improves understanding. *Cognitive science*, 18(3):439–477, 1994. 1

[14] Ganqu Cui, Yuchen Zhang, Jiacheng Chen, Lifan Yuan, Zhi Wang, Yuxin Zuo, Haozhan Li, Yuchen Fan, Huayu Chen, Weize Chen, et al. The entropy mechanism of reinforcement learning for reasoning language models. *arXiv preprint arXiv:2505.22617*, 2025. 2

[15] Yuhao Dong, Zuyan Liu, Hai-Long Sun, Jingkang Yang, Winston Hu, Yongming Rao, and Ziwei Liu. Insight-v: Exploring long-chain visual reasoning with multimodal large language models. In *Proceedings of the Computer Vision and Pattern Recognition Conference*, pages 9062–9072, 2025. 2

[16] Kaituo Feng, Kaixiong Gong, Bohao Li, Zonghao Guo, Yibing Wang, Tianshuo Peng, Junfei Wu, Xiaoying Zhang, Benyou Wang, and Xiangyu Yue. Video-r1: Reinforcing video reasoning in mllms. *arXiv preprint arXiv:2503.21776*, 2025. 5, 2

[17] Chaoyou Fu, Yuhuan Dai, Yongdong Luo, Lei Li, Shuhuai Ren, Renrui Zhang, Zihan Wang, Chenyu Zhou, Yunhang Shen, Mengdan Zhang, et al. Video-mme: The first-ever comprehensive evaluation benchmark of multi-modal llms in video analysis. In *Proceedings of the Computer Vision and Pattern Recognition Conference*, pages 24108–24118, 2025. 5, 2

[18] Daya Guo, Dejian Yang, Haowei Zhang, Junxiao Song, Ruoyu Zhang, Runxin Xu, Qihao Zhu, Shirong Ma, Peiyi Wang, Xiao Bi, et al. Deepseek-r1: Incentivizing reasoning capability in llms via reinforcement learning. *arXiv preprint arXiv:2501.12948*, 2025. 2, 1

[19] Yunzhuo Hao, Jiawei Gu, Huichen Will Wang, Linjie Li, Zhengyuan Yang, Lijuan Wang, and Yu Cheng. Can mllms reason in multimodality? emma: An enhanced multimodal reasoning benchmark. In *Forty-second International Conference on Machine Learning*. 5, 1

[20] Jujie He, Jiacai Liu, Chris Yuhao Liu, Rui Yan, Chaojie Wang, Peng Cheng, Xiaoyu Zhang, Fuxiang Zhang, Jiacheng Xu, Wei Shen, et al. Skywork open reasoner 1 technical report. *arXiv preprint arXiv:2505.22312*, 2025. 2

[21] hiyouga. Mathruler. <https://github.com/hiyouga/MathRuler>, 2025. 5

[22] Jingcheng Hu, Yinmin Zhang, Qi Han, Dixin Jiang, Xiangyu Zhang, and Heung-Yeung Shum. Open-reasoner-zero: An open source approach to scaling up reinforcement learning

on the base model. *arXiv preprint arXiv:2503.24290*, 2025. 2

[23] Kairui Hu, Penghao Wu, Fanyi Pu, Wang Xiao, Yuanhan Zhang, Xiang Yue, Bo Li, and Ziwei Liu. Video-mmmu: Evaluating knowledge acquisition from multi-discipline professional videos. *arXiv preprint arXiv:2501.13826*, 2025. 5, 2

[24] Yushi Hu, Weijia Shi, Xingyu Fu, Dan Roth, Mari Ostendorf, Luke Zettlemoyer, Noah A Smith, and Ranjay Krishna. Visual sketchpad: Sketching as a visual chain of thought for multimodal language models. *Advances in Neural Information Processing Systems*, 37:139348–139379, 2024. 2

[25] Wenxuan Huang, Bohan Jia, Zijie Zhai, Shaosheng Cao, Zheyu Ye, Fei Zhao, Zhe Xu, Yao Hu, and Shaohui Lin. Vision-r1: Incentivizing reasoning capability in multimodal large language models. *arXiv preprint arXiv:2503.06749*, 2025. 1, 2, 5

[26] Drew A Hudson and Christopher D Manning. Gqa: A new dataset for real-world visual reasoning and compositional question answering. In *Proceedings of the IEEE/CVF conference on computer vision and pattern recognition*, pages 6700–6709, 2019. 3

[27] David R Hunter. Mm algorithms for generalized bradley-terry models. *The annals of statistics*, 32(1):384–406, 2004. 2

[28] Aaron Hurst, Adam Lerer, Adam P Goucher, Adam Perelman, Aditya Ramesh, Aidan Clark, AJ Ostrow, Akila Welihinda, Alan Hayes, Alec Radford, et al. Gpt-4o system card. *arXiv preprint arXiv:2410.21276*, 2024. 1, 5

[29] Harsh Jhamtani and Taylor Berg-Kirkpatrick. Learning to describe differences between pairs of similar images. *arXiv preprint arXiv:1808.10584*, 2018. 3

[30] Mengzhao Jia, Wenhao Yu, Kaixin Ma, Tianqing Fang, Zhihan Zhang, Siru Ouyang, Hongming Zhang, Dong Yu, and Meng Jiang. Leopard: A vision language model for text-rich multi-image tasks. *Transactions on Machine Learning Research*. 2, 3

[31] Dongfu Jiang, Xuan He, Huaye Zeng, Cong Wei, Max Ku, Qian Liu, and Wenhui Chen. Mantis: Interleaved multi-image instruction tuning. *Transactions on Machine Learning Research*. 5, 1, 2

[32] Justin Johnson, Bharath Hariharan, Laurens Van Der Maaten, Li Fei-Fei, C Lawrence Zitnick, and Ross Girshick. Clevr: A diagnostic dataset for compositional language and elementary visual reasoning. In *Proceedings of the IEEE conference on computer vision and pattern recognition*, pages 2901–2910, 2017. 3

[33] Aniruddha Kembhavi, Mike Salvato, Eric Kolve, Minjoon Seo, Hannaneh Hajishirzi, and Ali Farhadi. A diagram is worth a dozen images. In *European conference on computer vision*, pages 235–251. Springer, 2016. 3

[34] Hynek Kydlíček. Math-Verify: Math Verification Library. 5

[35] Bo Li, Yuanhan Zhang, Dong Guo, Renrui Zhang, Feng Li, Hao Zhang, Kaichen Zhang, Peiyuan Zhang, Yanwei Li, Ziwei Liu, et al. Llava-onevision: Easy visual task transfer. *Transactions on Machine Learning Research*. 5

[36] Feng Li, Renrui Zhang, Hao Zhang, Yuanhan Zhang, Bo Li, Wei Li, Zejun Ma, and Chunyuan Li. Llava-next-interleave: Tackling multi-image, video, and 3d in large multimodal models. *arXiv preprint arXiv:2407.07895*, 2024. 5, 2

[37] Junnan Li, Yongkang Wong, Qi Zhao, and Mohan S Kankanhalli. Dual-glance model for deciphering social relationships. In *Proceedings of the IEEE international conference on computer vision*, pages 2650–2659, 2017. 3

[38] Jian Li, Weiheng Lu, Hao Fei, Meng Luo, Ming Dai, Min Xia, Yizhang Jin, Zhenye Gan, Ding Qi, Chaoyou Fu, et al. A survey on benchmarks of multimodal large language models. *arXiv preprint arXiv:2408.08632*, 2024. 1

[39] Kunchang Li, Yali Wang, Yinan He, Yizhuo Li, Yi Wang, Yi Liu, Zun Wang, Jilan Xu, Guo Chen, Ping Luo, et al. Mvbench: A comprehensive multi-modal video understanding benchmark. In *Proceedings of the IEEE/CVF Conference on Computer Vision and Pattern Recognition*, pages 22195–22206, 2024. 5, 1

[40] Qingbin Li, Rongkun Xue, Jie Wang, Ming Zhou, Zhi Li, Xiaofeng Ji, Yongqi Wang, Miao Liu, Zheming Yang, Minghui Qiu, et al. Cure: Critical-token-guided re-concatenation for entropy-collapse prevention. *arXiv preprint arXiv:2508.11016*, 2025. 2

[41] Ji Lin, Hongxu Yin, Wei Ping, Pavlo Molchanov, Mohammad Shoeybi, and Song Han. Vila: On pre-training for visual language models. In *Proceedings of the IEEE/CVF conference on computer vision and pattern recognition*, pages 26689–26699, 2024. 5

[42] Tsung-Yi Lin, Michael Maire, Serge Belongie, James Hays, Pietro Perona, Deva Ramanan, Piotr Dollár, and C Lawrence Zitnick. Microsoft coco: Common objects in context. In *European conference on computer vision*, pages 740–755. Springer, 2014. 3

[43] Fuxiao Liu, Kevin Lin, Linjie Li, Jianfeng Wang, Yaser Yacoob, and Lijuan Wang. Mitigating hallucination in large multi-modal models via robust instruction tuning. *arXiv preprint arXiv:2306.14565*, 2023. 3

[44] Haotian Liu, Chunyuan Li, Yuheng Li, Bo Li, Yuanhan Zhang, Sheng Shen, and Yong Jae Lee. Llava-next: Improved reasoning, ocr, and world knowledge, 2024. 5

[45] Mingjie Liu, Shizhe Diao, Ximing Lu, Jian Hu, Xin Dong, Yejin Choi, Jan Kautz, and Yi Dong. Prorl: Prolonged reinforcement learning expands reasoning boundaries in large language models. *arXiv preprint arXiv:2505.24864*, 2025. 2

[46] Zichen Liu, Changyu Chen, Wenjun Li, Penghui Qi, Tianyu Pang, Chao Du, Wee Sun Lee, and Min Lin. Understanding r1-zero-like training: A critical perspective. *arXiv preprint arXiv:2503.20783*, 2025. 2

[47] Ziyu Liu, Yuhang Zang, Xiaoyi Dong, Pan Zhang, Yuhang Cao, Haodong Duan, Conghui He, Yuanjun Xiong, Dahua Lin, and Jiaqi Wang. Mia-dpo: Multi-image augmented direct preference optimization for large vision-language models. In *The Thirteenth International Conference on Learning Representations*, 2025. 2, 5

[48] Pan Lu, Ran Gong, Shibiao Jiang, Liang Qiu, Siyuan Huang, Xiaodan Liang, and Song-Chun Zhu. Inter-gps: Interpretable geometry problem solving with formal language and symbolic reasoning. *arXiv preprint arXiv:2105.04165*, 2021. 3

[49] Pan Lu, Liang Qiu, Jiaqi Chen, Tony Xia, Yizhou Zhao, Wei Zhang, Zhou Yu, Xiaodan Liang, and Song-Chun Zhu.

Iconqa: A new benchmark for abstract diagram understanding and visual language reasoning. *arXiv preprint arXiv:2110.13214*, 2021. 3

[50] Pan Lu, Swaroop Mishra, Tanglin Xia, Liang Qiu, Kai-Wei Chang, Song-Chun Zhu, Oyvind Tafjord, Peter Clark, and Ashwin Kalyan. Learn to explain: Multimodal reasoning via thought chains for science question answering. *Advances in Neural Information Processing Systems*, 35:2507–2521, 2022. 3

[51] Pan Lu, Hritik Bansal, Tony Xia, Jiacheng Liu, Chunyuan Li, Hannaneh Hajishirzi, Hao Cheng, Kai-Wei Chang, Michel Galley, and Jianfeng Gao. Mathvista: Evaluating math reasoning in visual contexts with gpt-4v, bard, and other large multimodal models. *CoRR*, 2023. 5, 2

[52] Maryanne Martin. Local and global processing: The role of sparsity. *Memory & Cognition*, 7(6):476–484, 1979. 1

[53] Fanqing Meng, Lingxiao Du, Zongkai Liu, Zhixiang Zhou, Quanfeng Lu, Daocheng Fu, Tiancheng Han, Botian Shi, Wenhui Wang, Junjun He, et al. Mm-eureka: Exploring the frontiers of multimodal reasoning with rule-based reinforcement learning. *arXiv preprint arXiv:2503.07365*, 2025. 3

[54] Fanqing Meng, Jin Wang, Chuanhao Li, Quanfeng Lu, Hao Tian, Tianshuo Yang, Jiaqi Liao, Xizhou Zhu, Jifeng Dai, Yu Qiao, et al. Mmiu: Multimodal multi-image understanding for evaluating large vision-language models. In *The Thirteenth International Conference on Learning Representations*, 2025. 1, 5

[55] David Navon. Forest before trees: The precedence of global features in visual perception. *Cognitive psychology*, 9(3): 353–383, 1977. 1

[56] Long Ouyang, Jeffrey Wu, Xu Jiang, Diogo Almeida, Carroll Wainwright, Pamela Mishkin, Chong Zhang, Sandhini Agarwal, Katarina Slama, Alex Ray, et al. Training language models to follow instructions with human feedback. *Advances in neural information processing systems*, 35:27730–27744, 2022. 2

[57] Viorica Patraucean, Lucas Smaira, Ankush Gupta, Adria Recasens, Larisa Markeeva, Dylan Banarse, Skanda Koppula, Mateusz Malinowski, Yi Yang, Carl Doersch, et al. Perception test: A diagnostic benchmark for multimodal video models. *Advances in Neural Information Processing Systems*, 36:42748–42761, 2023. 3

[58] Rafael Rafailev, Archit Sharma, Eric Mitchell, Christopher D Manning, Stefano Ermon, and Chelsea Finn. Direct preference optimization: Your language model is secretly a reward model. *Advances in neural information processing systems*, 36:53728–53741, 2023. 2

[59] Guangming Sheng, Chi Zhang, Zilingfeng Ye, Xibin Wu, Wang Zhang, Ru Zhang, Yanghua Peng, Haibin Lin, and Chuan Wu. Hybridflow: A flexible and efficient rlhf framework. *arXiv preprint arXiv: 2409.19256*, 2024. 2

[60] Mohit Shridhar, Jesse Thomason, Daniel Gordon, Yonatan Bisk, Winson Han, Roozbeh Mottaghi, Luke Zettlemoyer, and Dieter Fox. Alfred: A benchmark for interpreting grounded instructions for everyday tasks. In *Proceedings of the IEEE/CVF conference on computer vision and pattern recognition*, pages 10740–10749, 2020. 3

[61] Zhaochen Su, Peng Xia, Hangyu Guo, Zhenhua Liu, Yan Ma, Xiaoye Qu, Jiaqi Liu, Yanshu Li, Kaide Zeng, Zhengyuan Yang, et al. Thinking with images for multimodal reasoning: Foundations, methods, and future frontiers. *arXiv preprint arXiv:2506.23918*, 2025. 2

[62] Alane Suhr, Stephanie Zhou, Ally Zhang, Iris Zhang, Hua-jun Bai, and Yoav Artzi. A corpus for reasoning about natural language grounded in photographs. *arXiv preprint arXiv:1811.00491*, 2018. 3

[63] Kai Sun, Yushi Bai, Ji Qi, Lei Hou, and Juanzi Li. Mm-math: Advancing multimodal math evaluation with process evaluation and fine-grained classification. In *Findings of the Association for Computational Linguistics: EMNLP 2024*, pages 1358–1375, 2024. 5, 2

[64] Gemini Team, Rohan Anil, Sebastian Borgeaud, Jean-Baptiste Alayrac, Jiahui Yu, Radu Soricu, Johan Schalkwyk, Andrew M Dai, Anja Hauth, Katie Millican, et al. Gemini: a family of highly capable multimodal models. *arXiv preprint arXiv:2312.11805*, 2023. 5

[65] Kimi Team, Angang Du, Bofei Gao, Bowei Xing, Changjiu Jiang, Cheng Chen, Cheng Li, Chenjun Xiao, Chenzhuang Du, Chonghua Liao, et al. Kimi k1. 5: Scaling reinforcement learning with llms. *arXiv preprint arXiv:2501.12599*, 2025. 2

[66] Fei Wang, Xingyu Fu, James Y Huang, Zekun Li, Qin Liu, Xiaogeng Liu, Mingyu Derek Ma, Nan Xu, Wenxuan Zhou, Kai Zhang, et al. Muirbench: A comprehensive benchmark for robust multi-image understanding. In *The Thirteenth International Conference on Learning Representations*, 2025. 1, 5

[67] Jiaqi Wang, Hanqi Jiang, Yiheng Liu, Chong Ma, Xu Zhang, Yi Pan, Mengyuan Liu, Peiran Gu, Sichen Xia, Wenjun Li, et al. A comprehensive review of multimodal large language models: Performance and challenges across different tasks. *arXiv preprint arXiv:2408.01319*, 2024. 1

[68] Ke Wang, Junting Pan, Weikang Shi, Zimu Lu, Houxing Ren, Aojun Zhou, Mingjie Zhan, and Hongsheng Li. Measuring multimodal mathematical reasoning with math-vision dataset. *Advances in Neural Information Processing Systems*, 37:95095–95169, 2024. 5, 2

[69] Peijie Wang, Zhong-Zhi Li, Fei Yin, Dekang Ran, and Cheng-Lin Liu. Mv-math: Evaluating multimodal math reasoning in multi-visual contexts. In *Proceedings of the Computer Vision and Pattern Recognition Conference*, pages 19541–19551, 2025. 5, 1

[70] Qi Wang, Yanrui Yu, Ye Yuan, Rui Mao, and Tianfei Zhou. Videorf: Incentivizing video reasoning capability in mllms via reinforced fine-tuning. *arXiv preprint arXiv:2505.12434*, 2025. 5

[71] Shenzhi Wang, Le Yu, Chang Gao, Chujie Zheng, Shixuan Liu, Rui Lu, Kai Dang, Xionghui Chen, Jianxin Yang, Zhenru Zhang, et al. Beyond the 80/20 rule: High-entropy minority tokens drive effective reinforcement learning for llm reasoning. *arXiv preprint arXiv:2506.01939*, 2025. 2

[72] Yaoting Wang, Shengqiong Wu, Yuecheng Zhang, Shuicheng Yan, Ziwei Liu, Jiebo Luo, and Hao Fei. Multimodal chain-of-thought reasoning: A comprehensive survey. *arXiv preprint arXiv:2503.12605*, 2025. 1

[73] Bo Wu, Shoubin Yu, Zhenfang Chen, Joshua B Tenenbaum, and Chuang Gan. Star: A benchmark for situated reasoning in real-world videos. *arXiv preprint arXiv:2405.09711*, 2024. 3

[74] Junbin Xiao, Xindi Shang, Angela Yao, and Tat-Seng Chua. Next-qa: Next phase of question-answering to explaining temporal actions. In *Proceedings of the IEEE/CVF conference on computer vision and pattern recognition*, pages 9777–9786, 2021. 3

[75] Shilin Xu, Yanwei Li, Rui Yang, Tao Zhang, Yueyi Sun, Wei Chow, Linfeng Li, Hang Song, Qi Xu, Yunhai Tong, et al. Mixed-r1: Unified reward perspective for reasoning capability in multimodal large language models. *arXiv preprint arXiv:2505.24164*, 2025. 5

[76] Semih Yagcioglu, Aykut Erdem, Erkut Erdem, and Nazli Ikizler-Cinbis. Recipeqa: A challenge dataset for multimodal comprehension of cooking recipes. In *Proceedings of the 2018 Conference on Empirical Methods in Natural Language Processing*, pages 1358–1368, 2018. 3

[77] Jianhao Yan, Yafu Li, Zican Hu, Zhi Wang, Ganqu Cui, Xiaoye Qu, Yu Cheng, and Yue Zhang. Learning to reason under off-policy guidance. *arXiv preprint arXiv:2504.14945*, 2025. 2

[78] Shuo Yang, Yuwei Niu, Yuyang Liu, Yang Ye, Bin Lin, and Li Yuan. Look-back: Implicit visual re-focusing in mllm reasoning. *arXiv preprint arXiv:2507.03019*, 2025. 2

[79] Yi Yang, Xiaoxuan He, Hongkun Pan, Xiyan Jiang, Yan Deng, Xingtao Yang, Haoyu Lu, Dacheng Yin, Fengyun Rao, Minfeng Zhu, et al. R1-onevision: Advancing generalized multimodal reasoning through cross-modal formalization. *arXiv preprint arXiv:2503.10615*, 2025. 1, 5

[80] Huanjin Yao, Jiaxing Huang, Wenhao Wu, Jingyi Zhang, Yibo Wang, Shunyu Liu, Yingjie Wang, Yuxin Song, Haocheng Feng, Li Shen, et al. Mulberry: Empowering mllm with o1-like reasoning and reflection via collective monte carlo tree search. *arXiv preprint arXiv:2412.18319*, 2024. 5

[81] Huanjin Yao, Qixiang Yin, Jingyi Zhang, Min Yang, Yibo Wang, Wenhao Wu, Fei Su, Li Shen, Minghui Qiu, Dacheng Tao, et al. R1-sharevl: Incentivizing reasoning capability of multimodal large language models via share-gpvo. *arXiv preprint arXiv:2505.16673*, 2025. 3

[82] Jiabo Ye, Haiyang Xu, Haowei Liu, Anwen Hu, Ming Yan, Qi Qian, Ji Zhang, Fei Huang, and Jingren Zhou. mplug-owl3: Towards long image-sequence understanding in multimodal large language models. In *The Thirteenth International Conference on Learning Representations*, 2025. 5

[83] Kexin Yi, Chuang Gan, Yunzhu Li, Pushmeet Kohli, Jiajun Wu, Antonio Torralba, and Joshua B Tenenbaum. Cleverer: Collision events for video representation and reasoning. *arXiv preprint arXiv:1910.01442*, 2019. 3

[84] Qiying Yu, Zheng Zhang, Ruofei Zhu, Yufeng Yuan, Xiaochen Zuo, Yu Yue, Weinan Dai, Tiantian Fan, Gaohong Liu, Lingjun Liu, et al. Dapo: An open-source llm reinforcement learning system at scale. *arXiv preprint arXiv:2503.14476*, 2025. 2, 4, 1

[85] Xiang Yue, Tianyu Zheng, Yuansheng Ni, Yubo Wang, Kai Zhang, Shengbang Tong, Yuxuan Sun, Botao Yu, Ge Zhang, Huan Sun, et al. Mmmu-pro: A more robust multi-discipline multimodal understanding benchmark. *arXiv preprint arXiv:2409.02813*, 2024. 5, 2

[86] Weihao Zeng, Yuzhen Huang, Wei Liu, Keping He, Qian Liu, Zejun Ma, and Junxian He. 7b model and 8k examples: Emerging reasoning with reinforcement learning is both effective and efficient. <https://hkust-nlp.notion.site/simplerl-reason>, 2025. Notion Blog. 2

[87] Chi Zhang, Feng Gao, Baoxiong Jia, Yixin Zhu, and Song-Chun Zhu. Raven: A dataset for relational and analogical visual reasoning. In *Proceedings of the IEEE/CVF conference on computer vision and pattern recognition*, pages 5317–5327, 2019. 3

[88] Guanghao Zhang, Tao Zhong, Yan Xia, Zhelun Yu, Haoyuan Li, Wanggui He, Fangxun Shu, Mushui Liu, Dong She, Yi Wang, et al. Cmmcot: Enhancing complex multi-image comprehension via multi-modal chain-of-thought and memory augmentation. *arXiv preprint arXiv:2503.05255*, 2025. 5

[89] Juntian Zhang, Yuhan Liu, Wei Liu, Jian Luan, Rui Yan, et al. Weaving context across images: Improving vision-language models through focus-centric visual chains. *arXiv preprint arXiv:2504.20199*, 2025. 1, 2, 5

[90] Bingchen Zhao, Yongshuo Zong, Letian Zhang, and Timothy Hospedales. Benchmarking multi-image understanding in vision and language models: Perception, knowledge, reasoning, and multi-hop reasoning. *arXiv preprint arXiv:2406.12742*, 2024. 5, 1

[91] Yaowei Zheng, Richong Zhang, Junhao Zhang, Yanhan Ye, Zheyuan Luo, Zhangchi Feng, and Yongqiang Ma. LlamaFactory: Unified Efficient Fine-Tuning of 100+ Language Models. Association for Computational Linguistics, 2024. 2

[92] Yaowei Zheng, Junting Lu, Shenzhi Wang, Zhangchi Feng, Dongdong Kuang, and Yuwen Xiong. Easyl1: An efficient, scalable, multi-modality rl training framework. <https://github.com/hiyouga/EasyR1>, 2025. 2

Mimic Human Cognition, Master Multi-Image Reasoning: A Meta-Action Framework for Enhanced Visual Understanding

Supplementary Material

7. Background: DAPO

DAPO [84] is an improved variant of GRPO [18], which directly computes the advantage A_t using the average reward over multiple sampled outputs, thereby eliminating the need for a separate value function as in PPO. Specifically, given a prompt $\mathbf{q} \sim P(Q)$, we sample G rollouts $\{\mathbf{o}_i\}_{i=1}^G$ from the current policy $\pi_{\theta_{\text{old}}}$. At each token position t in rollout i , the likelihood ratio is defined in Eq. 3.

$$r_{i,t}(\theta) = \frac{\pi_{\theta}(o_{i,t} | \mathbf{q}, \mathbf{o}_{i,<t})}{\pi_{\theta_{\text{old}}}(o_{i,t} | \mathbf{q}, \mathbf{o}_{i,<t})} \quad (3)$$

The group-relative advantage $\hat{A}_{i,t}$ is then obtained by standardizing each return R_i within the group, defined in Eq. 4.

$$\hat{A}_{i,t} = \frac{R_i - \text{Mean}(\{R_j\}_{j=1}^G)}{\text{Std}(\{R_j\}_{j=1}^G)}. \quad (4)$$

In contrast to GRPO, DAPO introduces several methodological advancements. Specifically, it employs a Clip-Higher mechanism, wherein ϵ_{high} is set greater than ϵ_{low} to enhance exploratory behavior; integrates Dynamic Sampling to systematically exclude data instances lacking informative learning signals; incorporates an Overlong Punishment strategy to constrain excessively verbose outputs; and adopts a Token-level Loss formulation to mitigate the inherent bias between responses of varying lengths. The training then proceeds by maximizing the clipped surrogate objective, defined for DAPO as follows:

$$\begin{aligned} \mathcal{J}_{\text{DAPO}}(\theta) = & \mathbb{E}_{(q,a) \sim \mathcal{D}, \{\mathbf{o}_i\}_{i=1}^G \sim \pi_{\theta_{\text{old}}}(\cdot | q)} \\ & \left[\frac{1}{\sum_{i=1}^G |\mathbf{o}_i|} \sum_{i=1}^G \sum_{t=1}^{|\mathbf{o}_i|} \min \left(r_{i,t}(\theta) \hat{A}_{i,t}, \right. \right. \\ & \left. \left. \text{clip}(r_{i,t}(\theta), 1 - \epsilon_{\text{low}}, 1 + \epsilon_{\text{high}}) \hat{A}_{i,t} \right) \right], \\ \text{s.t. } & 0 < |\{o_i \mid \text{is_equivalent}(R_i, 1)\}| < G. \end{aligned} \quad (5)$$

8. Benchmark

This section provides a detailed description of the benchmark used for evaluation.

MUIR MUIRBENCH [66] is a comprehensive benchmark designed for robustly evaluating MLLMs' multi-

image understanding capabilities. It comprises 11,264 images and 2,600 multiple-choice questions (average 4.3 images per instance), covering 12 diverse multi-image tasks (e.g., action understanding, cartoon storytelling, geographic map reasoning, 3D object multiview retrieval).

MMIU The Multimodal Multi-image Understanding (MMIU) [54] is a comprehensive benchmark tailored for evaluating MLLMs on multi-image comprehension tasks. Structured around cognitive psychology, it enumerates 7 types of multi-image relationships (refined from semantic, temporal, spatial categories) and covers 52 diverse tasks (e.g., multi-view action recognition, 3D object detection). In terms of scale, MMIU includes 77,659 images (2–32 per instance, averaging 6.64) and 11,698 meticulously curated multiple-choice questions.

MV-MATH MV-MATH [69] is a specialized benchmark designed to evaluate MLLMs on mathematical reasoning in multi-visual contexts—addressing the gap in existing benchmarks that mostly focus on single images. It comprises 2,009 high-quality mathematical problems derived from real K-12 scenarios.

EMMA EMMA [19] is a benchmark designed to evaluate Multimodal LLMs on genuine cross-modal reasoning. Its 2,788 questions across math, physics, chemistry, and coding require integrated visual-textual understanding, preventing solutions based on shallow cues or text alone.

Mantis-Eval Mantis-Eval [31] is a benchmark dataset designed to evaluate a model's ability to reason across multiple images. It contains 217 challenging examples.

MIRB MIRB [90] is a dedicated dataset addressing the gap in evaluating vision-language models (VLMs) on multi-image understanding, as existing benchmarks focus primarily on single-image inputs. It encompasses 925 samples across four core dimensions: perception, visual world knowledge, reasoning, and multi-hop reasoning, with all tasks requiring cross-comparison of multiple images (ranging from 2 to 42, averaging 3.78 per question).

MVBench MVBench [39] is a multi-modal video benchmark addressing the lack of temporal understanding evalu-

ation in MLLMs, covering 20 multi-frame-dependent video tasks (defined via a static-to-dynamic method). It is built efficiently by auto-converting public video annotations into multiple-choice QA (with ground-truth for fairness), reveals existing MLLMs’ poor temporal understanding.

Video-MME Video-MME [17] is the first comprehensive benchmark designed to evaluate MLLMs in video analysis. It fills the gap in assessing the understanding of sequential visual data by featuring 900 videos (ranging from 11 seconds to 1 hour) across 6 core domains (e.g., Knowledge, Sports Competition) and 30 subfields. Each video is paired with three expert-annotated multiple-choice QA pairs, resulting in a total of 2,700 questions. To support multi-modal reasoning, the benchmark also provides subtitles for 744 videos and audio tracks for all 900 videos.

Video-MMMU Video-MMMU [23] is a benchmark designed to evaluate the knowledge acquisition capabilities of MLLMs from professional video content. It comprises 300 expert-level videos spanning six disciplines and 30 sub-fields, paired with 900 human-annotated question–answer pairs. The benchmark measures performance across three cognitive stages: (1) *Perception*, assessing whether models can extract salient knowledge-related details from video content; (2) *Comprehension*, evaluating the ability to grasp and reason about the underlying concepts; and (3) *Adaptation*, examining whether models can transfer the acquired knowledge to novel or unfamiliar scenarios.

MMMU-Pro MMMU-Pro [85] is an enhanced version of the MMMU benchmark, designed to more rigorously evaluate multimodal models’ understanding and reasoning.

M3CoT M3CoT [9] addresses gaps in existing MCoT benchmarks (lack of visual reliance, single-step reasoning, limited domains) by enabling multi-domain, multi-step, multi-modal reasoning across 3 domains (science, mathematics, commonsense), 17 topics, and 263 categories. It has 11,459 total samples (7,973 train, 1,127 dev, 2,359 test) with diverse image types (geographic graphs, health images, etc.).

MM-MATH MM-MATH[63]consists of 5,929 open-ended middle school math problems paired with visual contexts, and it adopts fine-grained classification covering three dimensions: difficulty, grade level, and knowledge points.

MathVista MathVista [51] is proposed as a benchmark integrating challenges from mathematical and visual tasks.

It contains 6,141 examples, sourced from 28 existing multi-modal math datasets and 3 new ones (IQTest, FunctionQA, PaperQA), requiring fine-grained visual understanding and compositional reasoning—tasks that state-of-the-art foundation models find challenging.

MATH-V MATH-V [68] is a curated dataset designed to address the limited question diversity and subject breadth of existing visual math reasoning benchmarks. It comprises 3,040 high-quality math problems with visual contexts, all sourced from real math competitions.

9. Training Data Construction

For the construction of the training dataset, we referenced Mantis [31], LLaVA-Interleave [36], Leopard [30], and VideoR1 [16]. Overall, our dataset consists of multi-image data and single-image data, with 57k samples for cold-start training and 58k samples for RL. The detailed dataset statistics are presented in Table 1. Regarding the partitioning criteria for RL data and cold-start data, the key distinction between our cold-start and reinforcement learning dataset splits lies in the trajectory generation process described in Section 3.2. Cold-start training data consists of problems where GPT-4o successfully provides correct answers during Step 2, and for these instances, we proceed to Step 3 (retrieval-based diverse sampling) to obtain two distinct correct reasoning trajectories per problem that serve as supervised learning targets for cold start training. In contrast, reinforcement learning data comprises problems where GPT-4o fails to produce correct answers during Step 2, and these challenging cases are reserved for reinforcement learning.

10. Implementation

Our SFT experiments are primarily conducted using the LLaMA Factory framework [91], with the main hyperparameters summarized in Table 6. For the RL stage, we rely on the EasyR1 framework [92], a multi-model large-scale training system built upon VERL [59], and the key parameters are reported in Table 7. The experiments run on 32 A800 GPUs.

11. Case Study

Here we present a case study of our model in Figure 5 and 6, covering multi-image benchmarks, video benchmarks, and single-image benchmarks. The results demonstrate that, across different types of tasks, our model can dynamically invoke appropriate meta-actions to analyze the problem and produce correct answers.

Type	Dataset	Count for SFT	Count for RL
Multi-Image	ChartVQA[30]	2501	-
	SlideVQA[30]	3249	3000
	ALFRED[60]	8357	2754
	Nuscenes[4]	-	4946
	RecipeQA[76]	8759	5069
	IconQA[49]	5315	3000
	nlvr2[62]	5424	1620
	Spot-the-Diff[29]	2248	2589
	LRV[43]	-	2993
	RAVEN[87]	-	3200
Video	Star[73]	5490	2754
	NextQA[74]	1193	3000
	Clevrer[83]	3047	4478
	Perception[57]	2964	2500
Single-Image	Clevr_cogen_a_train ¹	1506	-
	Clevr_CoGenT_TrainA_70K_Complex ²	1159	3000
	M3COT[9]	1147	-
	Share-GRPO[81]	1145	3000
	GEOQA_R1V_Train_8K ³	800	4816
	AI2D[33]	630	-
	MMK12[53]	442	3537
	Geometry3k[48]	317	1406
	ScienceQA[50]	259	-
	PISC[37]	244	-
	Geoqa+[5]	172	891
	GQA[26]	119	-
	CLEVR_v1.0[32]	118	-
	COCO[42]	78	-
	LRV[43]	-	3063

Table 5. Statistics of Training Data

¹https://huggingface.co/datasets/leonardPKU/clevr_cogen_a_train

²https://huggingface.co/datasets/MMInstruction/Clevr_CoGenT_TrainA_70K_Complex

³https://huggingface.co/datasets/leonardPKU/GEOQA_R1V_Train_8K



Question:

What is the correct order of the images? A: [0, 1, 2, 3]\nB: [1, 3, 2, 0]\nC: [3, 2, 1, 0]\nD: [1, 3, 0, 2]

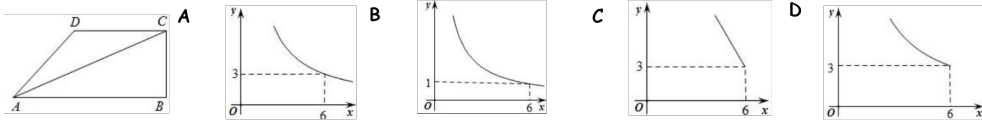
Response:

<global>Image2->cutting potatoes and onions->Image1, Image1->cooking the tomato-based mixture with chilies->Image4, Image4->adding tomatoes and seasoning to the pot->Image3</global>\n

(a) Case1.

Question:

As shown in the image, in quadrilateral $ABCD$, $\angle B=90^\circ$, $A C=6$, $A B \parallel C D$, and $A C$ bisects $\angle D$. Let $A B=x$ and $A D=y$. The graph that can roughly represent the functional relationship between y and x is ()

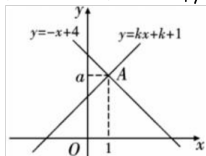


Response:

<global>Image1->analyze the geometry of quadrilateral $ABCD$ </global>\nABCD is given with $\angle B=90^\circ$, $AB \parallel CD$, and AC bisecting $\angle DAB$. This means we can use triangle similarity and trigonometric relationships to establish a functional relationship between x and y . Specifically, we need to calculate y based on x , and match the correct graph that represents this relationship. The key is to ensure that $y > 0$ and $x > 0$, and that $AC = 6$.</think>\n<hint>The critical point is to correctly analyze the geometry and establish the relationship y in terms of x . Since $AB \parallel CD$, we can use similar triangles to relate x and y . The graph must satisfy the constraints $y > 0$, $x > 0$, and the functional relationship derived must match one of the options provided. Pay attention to the shape and position of the graph relative to the axes and key points.</hint>\n<answer>D</answer>

(b) Case2.

Question: As shown in the figure, it is known that the graph of the linear function $y=kx+k+1$ intersects the graph of the linear function $y=-x+4$ at point $A(1, a)$. What are the values of a and k ?



Response:

<focus>The given images show two linear functions ($y = -x + 4$) and ($y = kx + k + 1$). The graphs intersect at point $A(1, a)$. The task is to find a and k .</focus>\nA(1, a) lies on $y = -x + 4$, substitute $x = 1$ into $y = -x + 4$: $y = -1 + 4 = 3$ $\Rightarrow a = 3$. 2. The point $A(1, 3)$ also lies on $y = kx + k + 1$. Substitute $x = 1$ and $y = 3$ into $y = kx + k + 1$: $3 = k + k + 1$ $\Rightarrow 3 = 2k + 1$ $\Rightarrow k = 1$.</think>\n<hint>The solution steps confirm that $a = 3$ and $k = 1$. Verify consistency of calculations for correctness.</hint>\n<focus>The calculations are consistent and logical. Ensure no arithmetic mistakes occurred during substitution and solving equations.</focus>\n<answer>a = 3 and k = 1.</answer>

(c) Case3.

Figure 5. Case study.

Question:
 In the AC circuit shown, the source voltage is _____ (1) V at an angle of _____ (2) degrees, and the difference between XL and XC is _____ (3) Ω . Please select from the following choices.
 A. 120, 45, 12 B. 60, 0, 12 C. 72, 0, 45 D. 45, 0, 72 E. 120, 0, 45 F. 60, 0, 72 G. 45, 0, 12 H. 72, 0, 60 I. 120, 0, 12 J. 120, 45, 72

Response:
 <global>Image1->introduce the topic of AC circuits and complex numbers->Image2, Image2->explain the concept of reactance and its components->Image3, Image3->illustrate how different elements react to current and voltage->Image4, Image4->introduce the phasor representation of AC voltage and current->Image5, Image5->show the AC circuit diagram and component placement->Image6, Image6->highlight the values of R , XL , and XC ->Image7, Image7->add the difference between XL and XC ->Image8, Image8->begin to calculate the resultant phasor->Image9, Image9->continue calculating the resultant phasor and write intermediate steps->Image10, Image10->finalize the calculation of Z and θ ->Image14</global>

 The AC circuit diagram in the images shows a source voltage of 120 V at an angle of 0° , with $R = 45 \Omega$, $XC = 60 \Omega$, and $XL = 72 \Omega$. The difference between XL and XC is 12Ω ($72 - 60 = 12$).</focus>

 The question asks for the source voltage, angle, and the difference in impedances. From the images, we can confirm that the source voltage is 120 V at 0° (AC 120 V $\angle 0^\circ$), and the difference between inductive reactance (XL) and capacitive reactance (XC) is 12Ω ($72 - 60 = 12$). By matching the options, we can select the correct values that fit the description.</think>

 </answer></case>

(a) Case4.

Question:
 Calculate the side widths and cross-sectional area of an embankment (Figure 11.13) having the following dimensions: Road width = 20 m, existing ground slope = 1 in 10 (10%); Side slopes = 1 in 2 (50%); centre height = 10 m. Please select from the following choices.
 A. Side width w_1 = 37.5 m, Side width w_2 = 25.5 m, Total area = 420.75 m^2 B. Side width w_1 = 37.3 m, Side width w_2 = 25.0 m, Total area = 418.75 m^2 C. Side width w_1 = 37.2 m, Side width w_2 = 25.0 m, Total area = 418.75 m^2 D. Side width w_1 = 37.2 m, Side width w_2 = 25.0 m, Total area = 418.75 m^2 E. Side width w_1 = 36.5 m, Side width w_2 = 24.5 m, Total area = 408.75 m^2 F. Side width w_1 = 38.0 m, Side width w_2 = 26.5 m, Total area = 425.75 m^2 G. Side width w_1 = 37.5 m, Side width w_2 = 25.0 m, Total area = 410.75 m^2 H. Side width w_1 = 37.5 m, Side width w_2 = 25.0 m, Total area = 418.75 m^2 I. Side width w_1 = 38.5 m, Side width w_2 = 26.0 m, Total area = 428.75 m^2 J. Side width w_1 = 37.0 m, Side width w_2 = 24.0 m, Total area = 415.75 m^2

Response:
 <global>Image7->introduce the formula for calculating width->Image8, Image8->provide values for height and side slope->Image9, Image9->calculate individual widths using formula->Image10, Image10->sum up to find total widths->Image12, Image12->introduce volume calculation using trapezoidal rule->Image13, Image13->perform volume calculation step by step->Image14</global>

 </focus>
 The key calculations involve determining the widths of the embankment using the formula $W = \frac{1}{2}(b + mh)$, where b is the formation width, h is the height, and m is the side slope. The total width is the average of the top and bottom widths. Additionally, the volume is calculated using the trapezoidal rule: $V = \frac{1}{3}(D_1 + 2D_2 + D_3)h$, where D_1, D_2, D_3 are areas at different levels, and D is the distance between levels.</focus>

 Using the formula $W = \frac{1}{2}(b + mh)$, calculate the widths for different levels:
 - For $h = 3.1$: $W_1 = \frac{1}{2}(6 + 3.1 \cdot 2) = 3.0 + 3.1 = 6.1$
 - For $h = 2.2$: $W_2 = \frac{1}{2}(6 + 2.2 \cdot 2) = 3.0 + 2.2 = 5.2$
 - For $h = 2.8$: $W_3 = \frac{1}{2}(6 + 2.8 \cdot 2) = 3.0 + 2.8 = 5.8$
 Sum the widths to find the total widths:
 $W_{\text{total}} = 6.1 + 5.2 + 5.8 = 17.1$
 Use the trapezoidal rule to calculate volume:
 $V = \frac{1}{3}(37.82 + 32.48 + 2(22.88)) \cdot 10 = 15 \cdot 116.06 = 1740.9$
 Match the calculated values to the options to find the correct one: H. The correct option must match $W_1 = 37.5$, $W_2 = 25.0$, $W_3 = 24.0$, and $V = 1740.9$. Option H satisfies these values with $W_1 = 37.5$, $W_2 = 25.0$, $W_3 = 24.0$, and $V = 1740.9$.</think>

 </answer></case>

(b) Case5.

Figure 6. Case study.

Parameter	Value
Model	
model_name_or_path	Qwen2.5-VL-7B-Instruct
image_max_pixels	100352
Method	
stage	sft
do_train	true
finetuning_type	full
Dataset	
template	qwen2_vl
cutoff_len	12000
overwrite_cache	true
preprocessing_num_workers	16
dataloader_num_workers	4
Train	
per_device_train_batch_size	1
gradient_accumulation_steps	4
learning_rate	1.0e-5
num_train_epochs	2
lr_scheduler_type	cosine
warmup_ratio	0.1

Table 6. Hyperparameters used in SFT.

Parameter	Value
Data	
max_prompt_length	4096
max_response_length	4096
rollout_batch_size	64
max_pixels	100352
min_pixels	50176
Algorithm	
adv_estimator	grpo
kl_coef	0.0
filter_groups_enable	true
filter_max_num_gen_batches	20
filter_metric	acc
Worker.Actor	
global_batch_size	32
max_grad_norm	1.0
entropy_coeff	0.0
kl_loss_coeff	0.0
clip_ratio_low	0.2
clip_ratio_high	0.28
optim.lr	1.0e-6
optim.weight_decay	1.0e-2
Worker.Rollout	
temperature	1.0
top_p	1.0
top_k	-1
n	8

Table 7. Hyperparameters used in RL.